energies

MDPI

Article

Microgrid Reliability Incorporating Uncertainty in Weather and Equipment Failure

Sakthivelnathan Nallainathan [1], Ali Arefi [1,*], Christopher Lund [1] and Ali Mehrizi-Sani [2]

[1] School of Engineering and Energy, Murdoch University, Perth, WA 6150, Australia; n.nallainathan@murdoch.edu.au (S.N.); c.lund@murdoch.edu.au (C.L.)
[2] The Bradley Department of Electrical and Computer Engineering, Virginia Tech, Blacksburg, VA 24061, USA; mehrizi@vt.edu
* Correspondence: a.arefi@murdoch.edu.au

Abstract: Solar photovoltaic (PV) and wind power generation are key contributors to the integration of renewable energy into modern power systems. The intermittent and variable nature of these renewables has a substantial impact on the power system's reliability. In time-series simulation studies, inaccuracies in solar irradiation and wind speed parameters can lead to unreliable evaluations of system reliability, ultimately resulting in flawed decision making regarding the investment and operation of energy systems. This paper investigates the reliability deviation due to modeling uncertainties in a 100% renewable-based system. This study employs two methods to assess and contrast the reliability of a standalone microgrid (SMG) system in order to achieve this goal: (i) random uncertainty within a selected confidence interval and (ii) splitting the cumulative distribution function (CDF) into five regions of equal probability. In this study, an SMG system is modeled, and loss of load probability (LOLP) is evaluated in both approaches. Six different sensitivity analysis studies, including annual load demand growth, are performed. The results from the simulations demonstrate that the suggested methods can estimate the reliability of a microgrid powered by renewable energy sources, as well as its probability of reaching certain levels of reliability.

Keywords: renewable energy; standalone microgrid; reliability evaluation; Monte Carlo simulation; cumulative distribution function

Received: 1 March 2025
Revised: 12 April 2025
Accepted: 15 April 2025
Published: 17 April 2025

Citation: Nallainathan, S.; Arefi, A.; Lund, C.; Mehrizi-Sani, A. Microgrid Reliability Incorporating Uncertainty in Weather and Equipment Failure. *Energies* **2025**, *18*, 2077. https://doi.org/10.3390/en18082077

1. Introduction

Reliability risk matrices, including loss of load probability (LOLP) and loss of load frequency (LOLF), are helpful in assessing system reliability from the supplier's point of view. In power system studies, these metrics can be evaluated either analytically or through simulation. However, when renewable energy resources are integrated, the analytical approach, which typically considers average failure rates and average load demand, becomes inadequate. This is because renewable resources exhibit significant variability, and relying solely on average values fails to capture the full range of fluctuations in generation and demand, leading to inaccurate reliability assessments [1]. As a result, the simulation approach has gained widespread popularity in recent years. When evaluating reliability risk matrices, time-series simulations with half-hourly or hourly sampling intervals are commonly employed. These reliability risk matrices provide valuable insights for decision making regarding reliability improvement initiatives, such as expanding installed capacity or optimizing resource allocation, to ensure the system can meet future demand and mitigate risks associated with renewable energy variability.

1.1. Reliability Indices and Evaluation Approaches

To assess the LOLP of a standalone microgrid (SMG) system, modeling and simulation of hourly power generation based on energy resource availability, such as solar irradiation and wind speed, is commonly utilized. Analytical approaches employ mathematical models to represent the system and produce reliability indices using probability theory solutions. In general, these methods are used to determine the average values of such indices. However, an average value provides limited insight into the variability of the reliability index. Probability distributions are used to address this issue and account for the variability inherent in the reliability index. The modeling process for the load and availability of energy resources should accurately depict their time-varying behavior, as well as any correlation between them. The positive correlation between energy resources and load has a substantial positive impact on microgrid reliability [2]. For example, load demand typically exhibits peak and off-peak periods throughout the day. However, relying on average daily demand fails to capture these fluctuations, potentially overlooking significant variations in load patterns that can influence system performance and reliability.

Hourly climate data such as solar irradiation and wind speed have a direct impact on renewable energy resource generation, such as solar PV and wind power. Consequently, the computation of solar radiation has a significant effect on a power system's LOLF and LOLP. Therefore, it is essential to investigate the extent of deviation or error in the loss of load probability (LOLP) calculation when different statistical approaches are employed to represent the uncertainties in solar irradiation and wind speed. This analysis will provide valuable insights into how varying methodologies impact the accuracy of reliability assessments in renewable energy systems. The aim of this research is to investigate the uncertainty of reliability evaluation methodologies, which eventually yield different reliability values for the same SMG system.

1.2. Literature Review

Many researchers assume that solar irradiation data from the previous year are representative of the current and future years [2,3]. Weather parameters evolve not only in the short term but also over extended periods due to factors such as climate change. For example, the solar irradiation at a specific hour in January 2021 may differ from the same hour in January 2022. Therefore, when evaluating system reliability over an operational lifespan of 20 to 25 years, it is essential to account for expected variations in weather parameters using robust statistical models. Relying solely on last year's climate data as a representation of future conditions is inadequate. Similarly, assuming that the average of data from previous years will accurately reflect future trends can lead to erroneous results. Dividing a year into generalized seasonal categories, such as hot cloudy days, cold cloudy days, hot sunny days, and cold sunny days [4], is not an accurate methodology, as it fails to capture the true daily variability of weather patterns. Furthermore, the use of various statistical distributions such as Weibull [5] and Gamma [6] is highly dependent on parameters such as scale, shape, and location. As a result, the precision of these statistical distributions is subjective [7]. The reliability of an SMG system is highly dependent on the statistical approach employed to model weather uncertainty [8–11]. This aspect is intuitively examined in this study.

Microgrid (MG) reliability evaluations are widely classified as analytical approaches, simulation methods, and hybrid methods. Reference [12] assessed the reliability of MG with significant renewable energy (RE) penetration using three different analytical methods: reliability block diagram (RBD), fault tree analysis (FTA), and the mission reliability method (MRM). Reference [2] used Monte Carlo simulation (MCS) to analyze the reliability of an SMG with stochastic generation and prioritized load, using five minutes of solar irradiation time-series data in the simulation. However, for reliability evaluation, this study assumed

the data were accurate and did not consider potential data uncertainty. Reference [7] assessed the reliability of an MG with renewable energy generation and load prioritization. This study used a Weibull distribution function to simulate wind speed and a Beta distribution function to model solar irradiation. Reference [13] presents a new MCS-based method for assessing reliability for operating distribution systems with multiple microgrids. In this study, they built a wind speed model utilizing historical data from the last sixty years, in which a wind speed time series of 6-hourly intervals from the preceding 60 years were fitted using a two-parameter Weibull distribution. The problem with this strategy is that there could be significant fluctuations in wind speed over six hours. Reference [14] used data from the preceding five years of solar irradiation and wind speed to mimic the probabilistic characteristics of solar and wind resources, and they assumed a 10% variance in power output from the model's nominal solar irradiance and wind speed. According to Reference [15], wind turbine generators and photovoltaic systems are less reliable than other types of regionally distributed resources since they are weather-dependent. Reference [16] employed a stochastic two-layer optimization method, which offers distinct advantages in managing energy system uncertainty and balancing the interests of multiple stakeholders in a power system network. Similarly, Reference [17] utilized a two-layer optimization model combined with a Conditional Value-at-Risk (CVaR)-based risk assessment approach, effectively addressing the uncertainty of complex energy systems while optimizing resource allocation. Reference [18] developed a linear optimization model to determine the benefits of electric vehicle (EV) smart charging on both network reliability improvement and electricity cost reduction. In the cost optimization framework, they included probabilistic aging failure constraints of transformers and transmission lines. In Reference [19], battery energy storage system (BESS) deterioration is described using two primary parameters: capacity fading and efficiency loss. Capacity fading causes a progressive loss in the battery's useable storage capacity over time. Efficiency loss reduces round-trip efficiency, which affects the battery's capacity to store and release energy effectively. Reference [20] presented a complete examination of uncertainties in power systems, including modeling, impact, and mitigation, which is critical for understanding and managing the issues in electric grids. In this paper, they stated that the existing literature lacks a comprehensive review and analysis of uncertainties in modern power systems, including uncertainties related to weather events, cyber-attacks, and asset management. Reference [21] provided a review on the issues of integrating solar power into isolated industrial microgrids with reliability constraints. The essential characteristics of reliability-constrained microgrids are defined, and a conceptual description is presented based on cutting-edge research from a variety of industrial applications. Reference [22] describes an approach for quantitatively assessing reliability and quantifying risk in microgrids while accounting for supply and demand variables. A new reliability indicator is presented, and a risk quantification method is devised to assess the likelihood of power deficiency under uncertainty. The suggested reliability assessment and risk quantification method is tested on an islanded hotel microgrid in Hong Kong. The findings suggest that the proposed reliability assessment approach can produce more robust reliability assessment results, whereas the conventional approach has an 8% chance of underestimating the maximum outage power. Reference [23] outlines microgrid energy management and forecasting uncertainties for renewable-based microgrid power systems. This study states that the uncertainty contained in microgrid systems must be considered for appropriate energy management. Monte Carlo simulation, the worst-case scenario approach, the point estimate method, the fuzzy method, and the autoregressive method have all been utilized recently to simulate uncertainty.

Reference [24] proposed a reliability cost–benefit analysis for the distribution system based on sequential MCS. The Markov model is used to analyze the reliability of the

transmission and distribution systems [25,26], Reference [25] used an analytical method to suggest a predicted reliability assessment of the distribution system, which included extreme weather circumstances. To compute the reliability indices, Reference [26] presented a one-step method based on a collection of binary descriptor matrices. Using an LOLP index, Reference [27] calculated the marginal cost of improving an SMG's reliability. In Reference [28], a hybrid probabilistic model for PV and wind was presented to test the robustness of a microgrid protection mechanism against weather intermittency. For the hybrid microgrid system design, Reference [29] used an yearly wind speed of 3.53 m/s and solar irradiation of 5.95 kWh/m^2/day. In all of these studies, the probabilistic consideration of resource availability, accounting for weather fluctuations, is not integrated with the probability of equipment failure.

In this study, the loss of load probability (LOLP) metric is employed to evaluate the system's reliability over a 25-year period (2021 to 2046). Time-series simulation studies typically incorporate hourly data on energy resources, such as solar irradiation, temperature, and wind speed, alongside hourly load demand. Simulating a 25-year horizon poses significant challenges, particularly in addressing uncertainties, such as inter-annual weather variability. Relying on seasonal trends or aggregated data, such as monthly or weekly averages, can help reduce uncertainty but oversimplifies the variability inherent in weather patterns. This approach fails to capture the dynamic nature of energy generation and consumption, leading to inaccuracies in assessing the reliability of the microgrid (MG) system. Therefore, an hourly time-series simulation is essential for accurately modeling the impact of weather variations and their influence on the system's LOLP. Such simulations provide a more precise and comprehensive analysis of system reliability, allowing for a deeper understanding of the interplay between renewable energy resources and load demand over extended periods. In the literature, either last year's data or the mean value of the previous few years' data is assumed to be the data for the entire 25-year simulation. This is not a reasonable assumption because it does not account for or illustrate the effects of global warming on climate change. This study sought to address this issue by modeling uncertainty using two distinct statistical approaches. Rather than attempting to forecast and derive data for a long period of time (25 years), the work presented in this paper proposed a method of randomly selecting a value for variables from a specific uncertainty range.

1.3. Research Contribution

According to the literature review, many researchers attempted to address resource uncertainty in SMG reliability evaluations, but only for a specific year. As a result, no researchers previously intended to evaluate the reliability of an SMG system over a 25-year lifespan while incorporating resource and equipment uncertainty in a time-series sequential simulation. Moreover, only a limited number of researchers have attempted to model the uncertainty of resources over multiple years. Consequently, the following are the key contributions of this paper:

- The development of a comprehensive model to incorporate weather uncertainties, including solar irradiation and wind speed, into the reliability assessment of microgrids with high renewable energy integration;
- The development of a methodology for designing a 100% renewable-based microgrid that accounts for weather uncertainties to ensure a specified level of reliability.

This paper is organized as follows: Section 2 presents the proposed methodology. Section 3 provides an in-depth explanation of the reliability evaluation algorithm. Section 4 discusses the case study, simulation process, and results. Finally, Section 5 concludes this study.

2. Proposed Research Methodology

In this work, two statistical methods are used to represent the uncertainty of renewable energy resources. They include the following:

- Introducing uncertainty through splitting the actual cumulative distribution function (CDF) into five equal-probability regions;
- Introducing uncertainty using a confidence interval.

The former is referred to as the real-CDF approach throughout this paper, while the latter is referred to as the confidence interval approach. Figure 1 depicts the step-by-step procedure for the two approaches used in this study. These two approaches were used to modify climate data from the past 30 years.

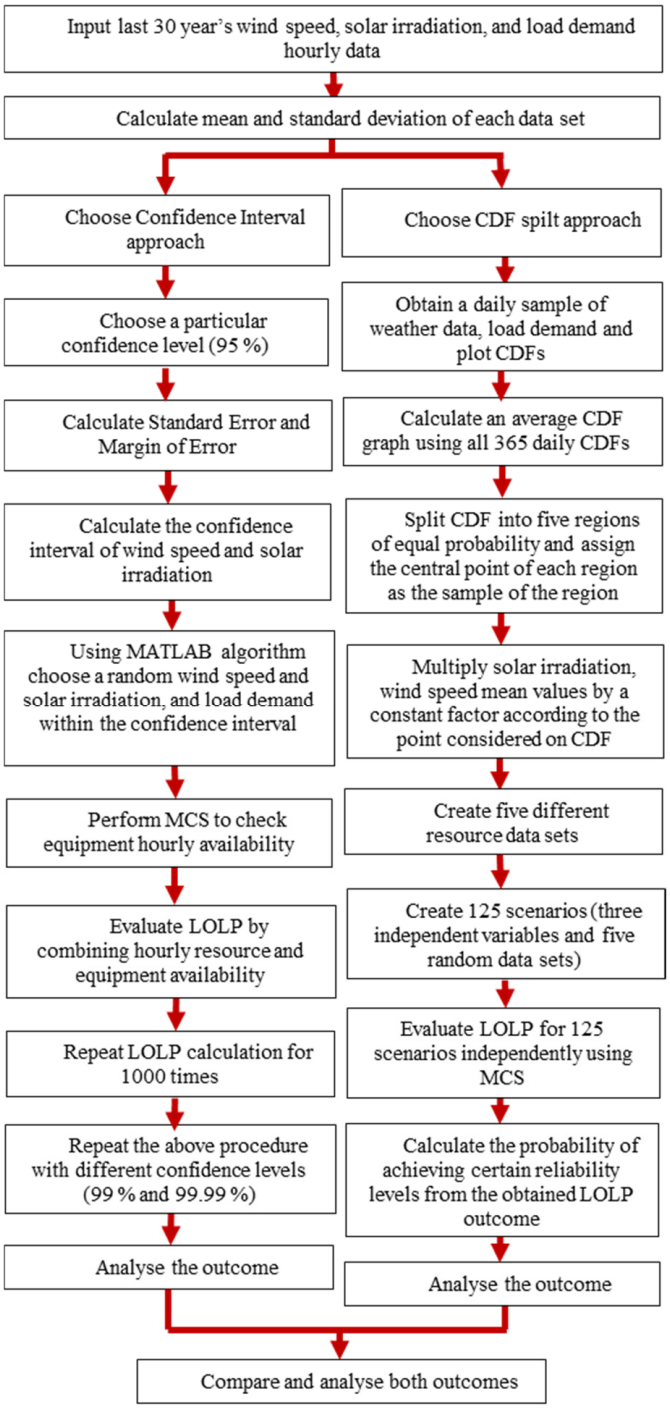

Figure 1. Flowchart of the proposed methodology.

The reliability of the SMG system will be examined using both approaches illustrated in Figure 1, and the results will be compared. Furthermore, an intuitive analysis is performed to determine why these two results differ. Finally, a conclusion is reached regarding the appropriate application of these two approaches. Essentially, the confidence interval approach addresses only a small variation in the data, whereas the real-CDF split approach incorporates a larger variation in the data. The simulation results are used to test these two aspects and their impact on reliability evaluation.

2.1. Introducing Uncertainty Using CDF Split Method

The uncertainty of resource availability is often modeled by segmenting the standard normal cumulative distribution function (CDF), with a mean of zero and a standard deviation of one, into five regions of equal probability. Each region is represented by its central point, which serves as the representative sample [30,31]. To incorporate this into simulations, the climate data are adjusted to create five distinct datasets, corresponding to these representative points on the CDF. This adjustment is achieved by scaling all variables in the climate data by a constant factor derived from the respective CDF point. However, this approach to accounting for uncertainty in solar irradiation is relatively simplistic. It can lead to unrealistic scenarios, such as excessively high solar irradiance values, which may not accurately reflect real-world conditions [30]. As a result, this method fails to accurately capture the year-to-year variability in climate data. Therefore, it is essential to determine the true distribution of resource data using hourly climate change data from the past 30 years. Preliminary research suggests that this approach better reflects resource uncertainty. For instance, over the last 30 years, solar irradiation in a given hour has ranged from 512 W/m^2 to 926 W/m^2. The proposed statistical model, referred to as the real-CDF approach, provides a range of values from 629 W/m^2 to 904 W/m^2, which more closely represents the actual variation in the data. In contrast, if a standard normal distribution (normal-CDF) is used, the model would show values between 761 W/m^2 and 864 W/m^2, reflecting a narrower range with less fluctuation. This narrower range does not accurately represent the true variation in climate data.

Data on resource availability, such as solar irradiation, ambient temperature, and wind speed at 12 p.m. (midday), are extracted from the past 30 years. A cumulative distribution function (CDF) is then plotted for each filtered dataset. These CDF plots represent daily resource uncertainty over the past 30 years, resulting in 365 individual CDF graphs. The average of these 365 CDFs is calculated to generate an overall average CDF plot, which summarizes the variation in resource availability. This approach forms the basis of the real-CDF methodology. Additionally, this procedure helps reduce the computational burden associated with generating 8760 individual CDF plots to represent hourly resource availability throughout the year. However, averaging all 8760 hourly CDF plots into a single CDF would be inaccurate, as solar irradiation data include zero values during night-time hours.

Figure 2 depicts the solar irradiation CDF graph at 12 p.m. (midday) on 1 January, using data from the previous 30 years. Figure 3 depicts the average CDF plot, which is the average value of 365 daily CDFs of solar irradiation based on 365 midday real-CDF samples. Figure 3 also shows how to identify five different coordinates that correspond to five different CDF regions. To divide the average real CDF into five equal-probability regions, y-axis is divided into five ranges of cumulative probability, namely, (0–0.2), (0.2–0.4), (0.4–0.6), (0.6–0.8), and (0.8–1.0), and the central point of each region, which are 0.1, 0.3, 0.5, 0.7, and 0.9, are marked as the representative sample [31,32]. The corresponding x-axis points are then identified using MATLAB R2020b tools. The average solar irradiation and wind speed of each hour are calculated using hourly climate data from the last 30 years.

This is calculated by adding all 30 years' *i*th hour solar irradiation and dividing the total value by 30. The result is termed as average climate data. These average climate data are then modified in the simulation study based on these five distinct x coordinate values (multipliers), yielding five distinct datasets. This is performed by multiplying all resource variables in the climate data by a constant factor. For example, in Figure 3, a CDF of 0.1 equals −1.688; if SD is the standard deviation corresponding to the *i*th hour of solar irradiation, the multiplication factor in the *i*th hour is $(1 + ((-1.688) \times SD))$. The SD is calculated for each hour in a year (using 30 different data points), for a total of 8760 SDs. Figure 4 shows the CDF wind speed graph at 12 p.m. (midday) from 1 January 1989 to 2019.

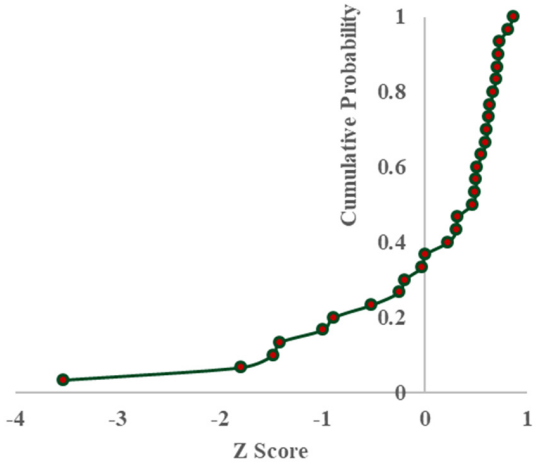

Figure 2. Cumulative distribution of solar irradiation for a particular hour over 30 years.

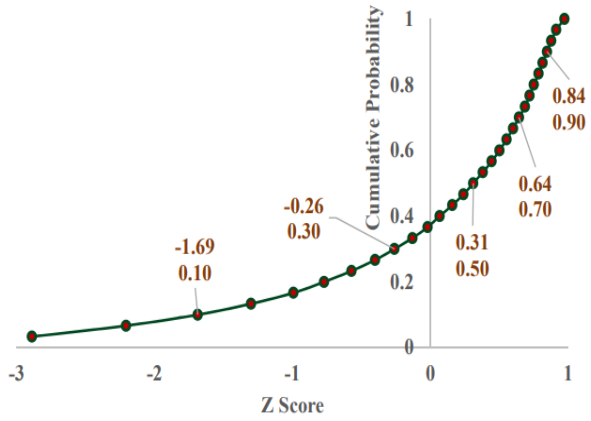

Figure 3. Average CDF graph.

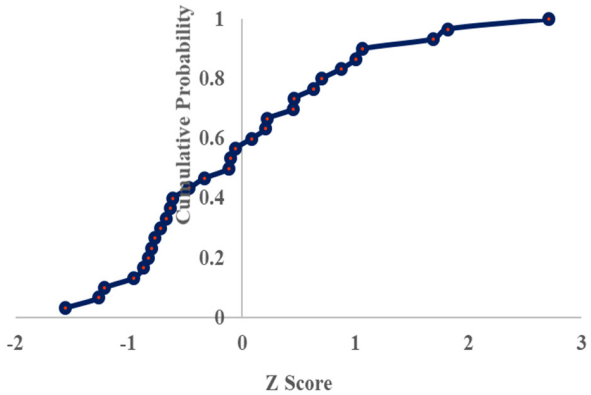

Figure 4. Variation in wind speed for a particular hour over 30 years.

Figure 5 illustrates the average CDF graph for wind speed, derived from the 365 daily CDFs of solar irradiation based on midday CDF samples. The Z-score represents the number of standard deviations away from the mean value of the reference population. In this study, the reference populations are wind speed and solar irradiation. Similarly, the CDF graphs for ambient temperature and load demand are plotted in the same manner, and their average CDFs are determined.

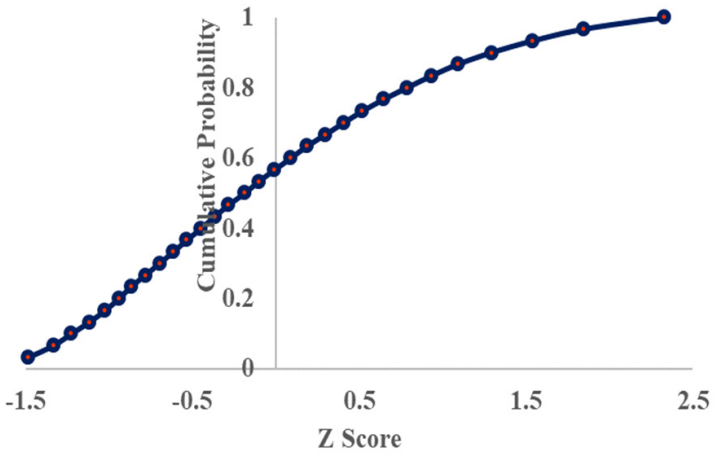

Figure 5. Wind speed average CDF graph.

In the real-CDF approach, the CDF curve is divided into five regions with equal probability, resulting in five distinct datasets. This means that variables such as solar irradiation, wind speed, and load demand each have five possible values for every iteration of the simulation. To select the solar irradiation value for the *i*th hour (where *i* represents any hour of the year, from 0 to 8760), the algorithm randomly selects one value from the five possible values. Additionally, solar irradiation, wind speed, and load demand are treated as independent variables. For example, during the *i*th hour, the MATLAB algorithm may select the minimum value of solar irradiation, the median value of wind speed, and the maximum value of load demand, each from their respective five possible values. As a result, the selection of resource and load demand values is a random process for each hour.

To select variables independently, a MATLAB algorithm is developed with 125 permutations based on three independent variables: solar irradiation, wind speed, and load demand, each with five possible values. This results in a total of 125 permutations. The algorithm randomly selects variable values from these permutations and computes the loss of load frequency (LOLF) for all possible combinations. Ambient temperature is also included in this study, but it is not treated as an independent variable. Instead, it follows the solar irradiation climate data. This means that when the MATLAB algorithm selects a multiplication factor for solar irradiation (for example, a multiplication factor equivalent to a CDF of 0.9), the ambient temperature also copies the same multiplication factor.

Using the following approach, the simulation results from the 125 permutations (125 scenarios) will be converted into probabilities. The probability of a specific event occurring is calculated by dividing the number of scenarios where the event occurs by the total number of scenarios (125). For example, if the event of achieving 99% reliability occurs in 10 out of the 125 scenarios, the probability is 8% (calculated as 10 divided by 125, multiplied by 100).

2.2. Introducing Uncertainty Using Confidence Interval

The average hourly values of solar irradiation, ambient temperature, and wind speed are calculated using climate data from the past 30 years. When three different confidence intervals (99.99%, 99%, and 95%) are selected, the data ranges for resource and load

demand will vary, resulting in three distinct spreads or deviations from the mean. A higher confidence interval, such as 99.99%, will produce a wider range (spread) compared to the lower confidence intervals. This larger range better reflects the true variation in the data. Consequently, the primary objective of this study is to evaluate the reliability of the SMG system by considering these three confidence intervals.

Calculating the mean value from the past 30 years of hourly load demand data is impractical, as the number of customers in the system can change over time, leading to fluctuations in demand. Therefore, the load demand data from the most recent year (2019) are used, with a 5% standard deviation applied. Using the MATLAB *rand* function, 30 different random load demands are then generated to account for variability in the system.

$$\overline{x} = \frac{\sum_{i=1}^{n} x_i}{n} \tag{1}$$

$$s = \sqrt{\frac{(x_i - \overline{x})^2}{n-1}} \tag{2}$$

$$SE_{mean} = \frac{s}{\sqrt{n}} \tag{3}$$

$$CI = \overline{x} \pm t_{n-1,\ \frac{\alpha}{2}} \,.\, SE_{mean} \tag{4}$$

where $\overline{x}$ is the mean value, x_i is the value of i^{th} variable, n is the total number of variables, and s is the sample's standard deviation. The mean and standard deviation of solar irradiance, temperature, and wind speed can be computed using (1) and (2), as in (3), where SE_{mean} is the standard error of mean. CI is the confidence interval, and $t_{n-1,\frac{\alpha}{2}}$ is the T-score at a given degree of freedom and level of significance, α. The level of significance can be calculated for a specific confidence interval selected. For instance, if confidence interval of 95% is chosen, then the level of significance becomes 0.05 (=1 − 0.95). An x % confidence interval is a rule-based interval that covers the true value x % of the time under simulated conditions [32]. When the population standard deviation is unknown, a T-score is used. In this study, we use hourly climate data from the last 30 years as a sample, with the true population's standard deviation unknown.

The MATLAB algorithm is designed to randomly select the hourly weather parameters within the range defined by the upper and lower bounds, which are determined using the chosen confidence interval. To generate the random values, a uniform distribution is used to ensure an even probability across the specified range:

$$r = a + rand(). (b - a) \tag{5}$$

where r is the value of the variable, a is the lower bound, b is the upper bound, and *rand* is the random function that generates random values between 0 and 1.

3. Reliability Evaluation

The reliability of the system is influenced by two key factors: the availability of equipment and the availability of renewable energy resources. To enhance the reliability of the SMG system, a holistic reliability evaluation method is essential. This method assesses the reliability level by evaluating the availability of generating resources, generating equipment, and distribution components on an hourly basis. A comprehensive mathematical model that integrates resource and equipment availability for each hour has been proposed in a previous study [3]. This approach ensures a thorough analysis of the system's reliability, accounting for both resource variability and equipment performance. The time to failure (TTF) value of each equipment type is calculated using MCS, which creates random

values. In this process, random prediction is used to achieve two goals: assessing the zero reliability or down state of the equipment and estimating the equipment's TTF in each hour. Non-sequential MCS is used to forecast failures. Using the state duration sampling approach, the reliability model of the PV, WT, BESS, and Microgrid Distribution Network (MGDN) reflecting equipment availability is generated. Weather characteristics such as solar radiation, ambient temperature, and wind speed are utilized to simulate hourly power output from renewable energy sources. Figure 6 depicts how the reliability of the MG system is dependent on the availability of equipment and resources; the arrows represent the direction of energy flow.

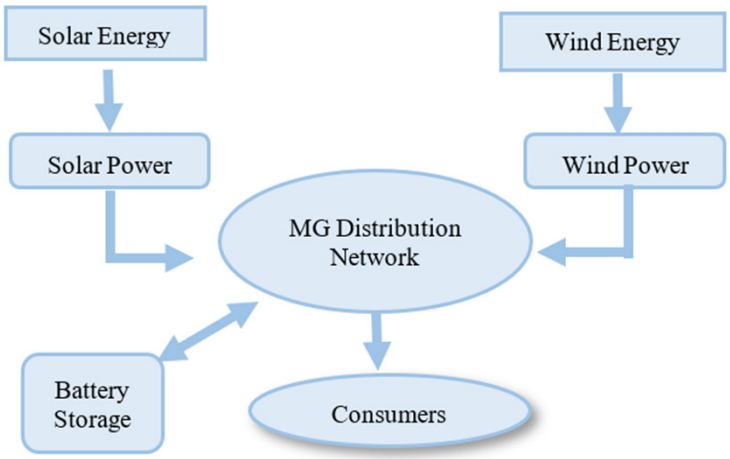

Figure 6. MG with equipment and resources.

3.1. Resource Availability Modeling

The availability of the components that are currently in operation determines the system's reliability at any given time. Thus, the hourly reliability value of MG is derived by establishing which energy sources are supplying electricity at the moment. The variable renewable energy resources WT, solar PV, and BESS run in parallel in this MG architecture, whereas the MG distribution network operates in series, as shown in Figure 6. The series and parallel components of the MG system will change every hour based on the amount of electricity produced.

If wind power generation, solar PV generation, and energy stored in the battery are individually greater than the load demand, then all these are considered as parallel, and the MG distribution network will be in series with this. R^R_{MG}, R_{WT}, R_{PV}, R_{BESS}, and R_{MGDN} represent the reliability of the microgrid system, reliability of the wind turbine, PV panel, battery energy storage system, and distribution network, respectively.

$$R^R_{MG} = (1 - (1 - R_{WT}).(1 - R_{PV}).(1 - R_{BESS}))R_{MGDN} \quad (6)$$

If wind power and solar PV generation are individually more than the load demand and the stored energy is insufficient to meet the load need, then wind and solar power generation are viewed as parallel components in this context. This is because, at this moment, either wind power or solar PV generation can meet the demand for load.

$$R^R_{MG} = (1 - (1 - R_{WT}).(1 - R_{PV}))R_{MGDN} \quad (7)$$

If only wind power generation is greater than the load demand and if the battery is fully charged but not sufficient to supply the load, then wind power generation alone can supply the load demand.

$$R^R_{MG} = R_{WT} \cdot R_{MGDN} \quad (8)$$

If wind and solar PV generation, together with battery energy storage, is greater than or equal to the load demand, then all the components are series in operation.

$$R_{MG}^{R} = R_{WT} \cdot R_{PV} \cdot R_{BESS} \cdot R_{MGDN} \quad (9)$$

3.1.1. Modeling of Renewable Energy Resources

Weather data, such as solar radiation and ambient temperature, are important factors in determining the electricity provided by solar PV. The wind power system's output power is determined by its wind velocity and power curve. Wind velocity measured by a meteorological station is used to simulate wind power generation.

3.1.2. Modeling of Battery Energy Storage System

To simulate the battery storage system, the excess power and power deficit of the MG system must be calculated for each hour. The excess power available in the MG system is utilized to charge the battery, and the remaining excess power will be curtailed. To decrease the complexity of this study, the BESS is modeled utilizing only excess and deficit energy, as well as installed capacity.

3.1.3. Loss of Load Calculation

In each hour, a loss of load (LOL) event occurs if resource unavailability is encountered. To illustrate, LOL occurs when the total power generated by renewable energy and stored power in the battery at the end of the previous hour is less than the power demand for the current hour.

$$\mathrm{LOL}^{\mathrm{i}} = 0 \quad \forall P_t^i + P_{BES}^{i-1} > P_L^i \quad (10)$$

$$\mathrm{LOL}^{\mathrm{i}} = 1 \quad \forall P_t^i + P_{BES}^{i-1} < P_L^i \quad (11)$$

where $\mathrm{LOL}^{\mathrm{i}}$ is the LOL event at the ith hour, P_t^i is the total renewable power generation at the ith hour, $+P_{BES}^{i-1}$ is the energy stored in the battery at $i-1$ h, and P_L^i is the total load demand at the ith hour.

3.1.4. Equipment Availability Modeling

In this study, four distinct types of equipment were considered: a solar PV array, a WT, a BESS, and the MG distribution network (MGDN). This study does not consider partially failed components; instead, component failure is believed to be a complete failure. Failure of 5 MW of PV panels, for example, indicates the failure of all cells in that panel. This is because the simulation algorithm used in this study does not account for partial equipment failure. This assumption is made to help simplify the suggested reliability evaluation approach.

The time to failure (TTF) value of each equipment type is calculated by generating random values. In this process, two elements are determined using random prediction: the zero reliability or down state of the equipment and the estimated TTF of the equipment each hour. Figure 7 depicts the transition of the components from the up to down state.

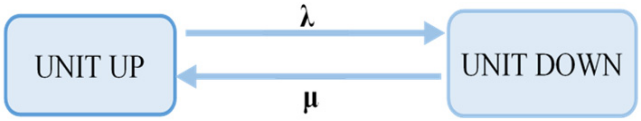

Figure 7. Two-stage reliability model. λ: failure rate, μ: repair rate.

Because this employs non-sequential MCS and is aimed at forecasting failure events, only the failure rate was analyzed, and repair time was excluded. The PV, WT, BESS,

and MGDN reliability models were created using a state duration sampling method. The following method can be used to calculate the time to failure (TTF):

Step 1: Generate 219,600 uniformly distributed random numbers (U~(0, 1)), representing the number of hours in 25 years.
Step 2: Compute the TTF using (12).

$$TTF = -MTTF \cdot ln(U) \tag{12}$$

Step 3: Repeat the above two steps to find the TTF of each equipment type, such as the solar PV array, wind turbine, battery, and MG network, separately.
Step 4: Identify which energy resources were supplying electricity to the load at each hour.
Step 5: Calculate the TTF of the system during each hour.

3.1.5. System Modeling

The MG system's reliability has been simulated using the following approach, which combines resource and equipment availability across each hour:

Step 1: Take the complement of the LOL event in each hour.

$$F^i = 1 \quad \forall LOL^i = 0 \tag{13}$$

$$F^i = 0 \quad \forall LOL^i = 1 \tag{14}$$

Step 2: Calculate the time to failure of the MG system using Equation (15), where TTF^i_{MG}, and TTF^i_E represent the time to failure of the microgrid system and the time to failure of the microgrid equipment in the ith hour.

$$TTF^i_{MG} = (TTF^{\,i}_{E})(\mathrm{F^i}) \tag{15}$$

4. Simulation Results and Discussion

The Results Section exhibits the simulation results obtained using two different statistical approaches: the real-CDF approach and the confidence interval approach. Various sensitivity analyses and their results are also discussed. Finally, the outcomes of these two approaches are compared.

4.1. Case Study

For this study, the load demand for the Aberdeen substation in New South Wales, Australia, was collected from the Ausgrid website, while hourly sun irradiation, ambient temperature, and wind speed statistics for this area were gathered from the website renewables.ninja. This case study examines aggregated load demand data collected for the year 2019, with a peak demand of 5.04 MW and a daily average demand of 3.72 MW.

The base case is built entirely from renewable energy sources. Renewable energy resources such as solar PV and WT, as well as battery energy storage systems (BESSs), are deployed with a capacity nearly double that of the SMG system's peak demand. As a result, the base scenario contains 10 megawatts of solar PV, 10 megawatts of wind power output, and 10 megawatt hours of battery storage. This study focuses on a lithium-ion battery. Figure 8 depicts the load profile of the Aberdeen substation. The load profile begins on 1 January 2019 and ends on 31 December 2019.

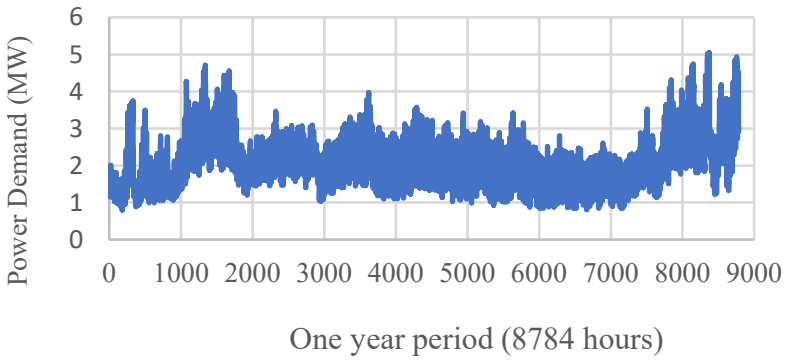

Figure 8. Load profile of the Aberdeen substation in the year 2019.

4.2. Split CDF into Five Regions of Equal Probability

In this section, reliability is evaluated by incorporating resource uncertainty into the real-CDF curve, which is divided into five equal-probability regions. The subsequent section examines 125 distinct scenarios and their corresponding reliability outcomes. This study considers three variables: solar energy resources, wind energy resources, and load demand. According to the real-CDF split method, each variable can independently select a value from a set of five options (derived from the real-CDF split). By combining the three variables with their five independent values, a total of 125 permutations, referred to as the 125 distinct scenarios, are generated. As a result, a simulation study with 1000 Monte Carlo simulations is conducted for each scenario, yielding 125 independent outcomes.

Figure 9 illustrates the PDF curve for the reliability values of the 125 scenarios. This PDF curve was created by rearranging the outcomes of all 125 scenarios in ascending order.

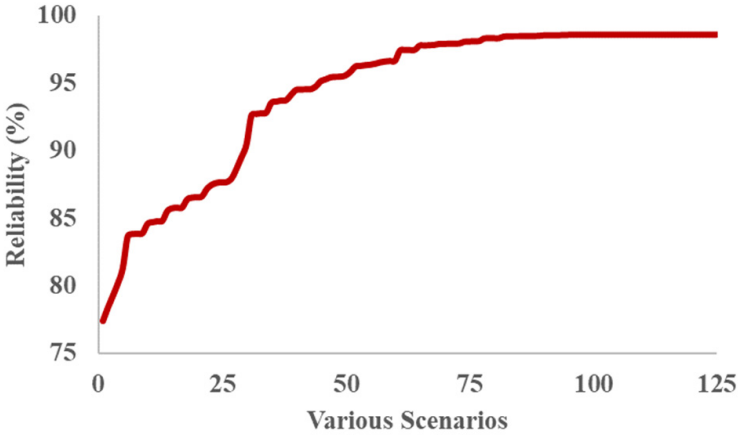

Figure 9. PDF curve representing reliability outcomes of 125 scenarios.

Table 1 presents the highest reliability values achieved using this evaluation approach. These values are observed when resource levels are higher (selected randomly within the given range by the MATLAB algorithm) and the load demand is lower. Under such conditions, the highest reliability value is expected.

Table 1. Highest possible reliability value (out of 125 scenarios).

	SMG System	SMG Resources Alone	SMG Equipment Alone
Reliability	98.67%	100%	98.67%
LOLP	1.33%	0%	1.33%
LOLF	2906	0	2906

Table 2 presents the lowest reliability value obtained using this evaluation method. As expected, the lowest reliability value occurs when resource levels are at their minimum and the load demand is at its maximum. Based on the data from Tables 1 and 2, the reliability of the SMG system ranges from 77.37% to 98.67%. This indicates a reliability uncertainty of 21.3%.

Table 2. Lowest possible reliability value (out of 125 scenarios).

	SMG System	SMG Resources Alone	SMG Equipment Alone
Reliability	77.37%	77.89%	98.59%
LOLP	22.63%	22.19%	1.41%
LOLF	49,552	48,425	3085

Calculating Probability of Achieving Target Reliability Levels

This approach evaluates 125 permutations, making it essential to determine how many scenarios meet specific reliability thresholds. For instance, if a reliability level of 97% is required, the number of permutations with a loss of load frequency (LOLF) of 6570 or lower must be counted. (A 1% unreliability corresponds to an LOLF of 2190, so a 3% unreliability equates to an LOLF of 6570.) Based on the simulation study results shown in Table 3, 66 out of the 125 scenarios achieve a reliability level of 97%.

Table 3. Total number of events achieving a specific reliability level.

Target Reliability	Required LOLF to Meet the Target Reliability	Number of Scenarios Which Meets the Required LOLF Criteria	Probability in Percentage
98.50%	3285	37	29.6%
98.25%	3833	48	38.4%
98.00%	4380	53	42.4%
97%	6570	66	52.8%
96%	8760	75	60%
95%	10,950	82	65.6%
94%	13,140	88	70.4%
93%	15,330	92	73.6%
92%	17,520	96	76.8%
91%	19,710	96	76.8%
90%	21,900	97	77.6%

Table 3 presents the number of occurrences and the corresponding probabilities for achieving specific reliability levels within the sample space of 125 scenarios. Figure 8 illustrates the likelihood of attaining various reliability levels. For example, the probability of achieving a 90% reliability level is 77.6%, while the probability of reaching 98.50% reliability is 29.6%.

Figure 10 illustrates the probability of obtaining specific reliability levels.

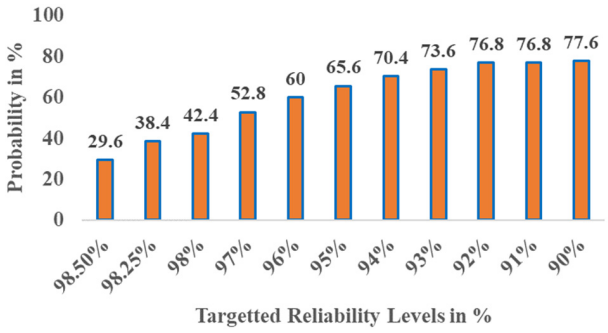

Figure 10. Probability of obtaining specific reliability levels.

4.3. Reliability Calculation Using Confidence Interval

The confidence interval provides a range of potential values for a given variable. In this section, uncertainty in energy resource availability is modeled using confidence intervals to account for variability and ensure a more accurate representation of resource fluctuations.

4.3.1. Confidence Level of 99.99%

This section discusses the simulation results obtained using a 99.99% confidence interval for the sample data, including solar irradiation, wind speed, and load demand. Table 4 summarizes the reliability values calculated with a 99.99% confidence interval, showing that the SMG system achieves an average reliability of 95.98%. Figure 11 illustrates the frequency of specific reliability levels across 1000 Monte Carlo simulations. The standard deviation of the simulation results is 0.0402. Figure 12 displays the probability density function (PDF) and cumulative distribution function (CDF) curves for SMG system reliability under a 99.99% confidence interval. These curves provide a detailed representation of how the reliability results from the 1000 simulations are distributed.

Table 4. Reliability of SMG system using 99.99% confidence interval.

	SMG System	SMG Resources Alone	SMG Equipment Alone
Reliability	95.98%	97.34%	98.59%
LOLP	4.02%	2.66%	1.41%
LOLF	8814	5815	3086

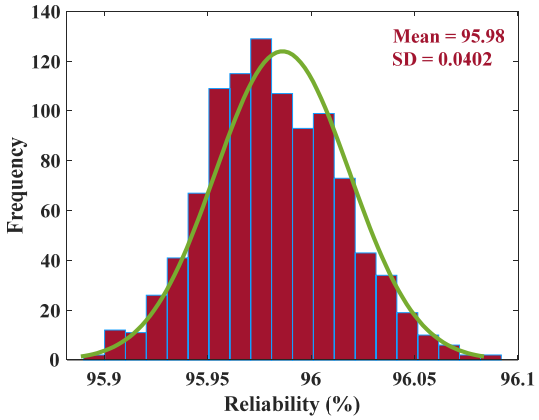

Figure 11. Frequency diagram of SMG reliability.

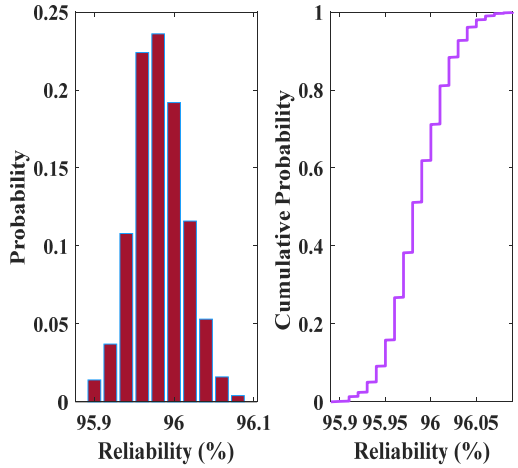

Figure 12. PDF and CDF of SMG system reliability with 99.99% confidence interval.

4.3.2. Confidence Level of 99.00%

This section examines the simulation results obtained using a 99% confidence interval for the sample data, including solar irradiation, wind speed, and load demand. Table 5 presents the reliability values calculated at the 99% confidence level, indicating that the SMG system achieves an average reliability of 96.86%. Figure 13 illustrates the probability density function (PDF) and cumulative distribution function (CDF) curves for SMG system reliability at the 99% confidence interval, offering a comprehensive view of the reliability distribution.

Table 5. Reliability of SMG system using 99% confidence interval.

	SMG System	SMG Resources Alone	SMG Equipment Alone
Reliability	96.86%	98.24%	98.59%
LOLP	3.14%	1.76%	1.41%
LOLF	6886	3858	3084

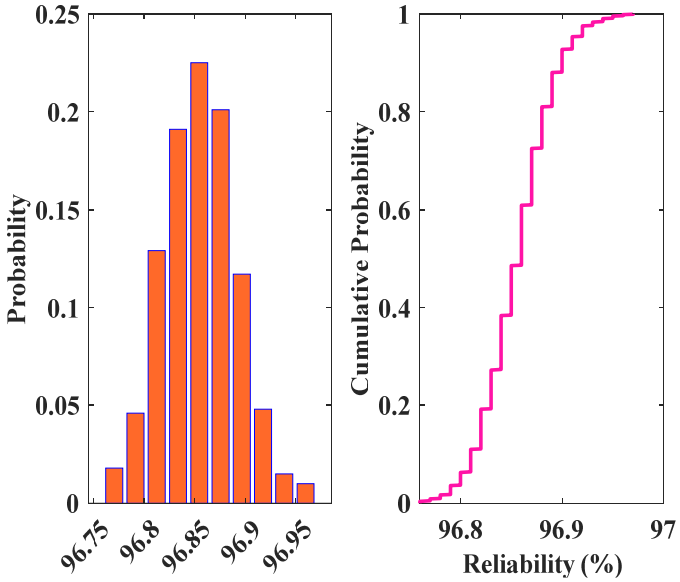

Figure 13. PDF and CDF of SMG system reliability.

4.3.3. Confidence Level of 95.00%

This section presents the simulation results obtained using a 95% confidence interval for the sample data, including solar irradiation, wind speed, and load demand. Table 6 outlines the reliability values at the 95% confidence level, showing that the SMG system achieves a reliability of 97.36%. Figure 14 illustrates the probability density function (PDF) and cumulative distribution function (CDF) curves for SMG system reliability under the 95% confidence interval, providing a detailed visualization of the reliability distribution.

Table 6. Reliability of SMG system using 95% confidence interval.

	SMG System	SMG Resources Alone	SMG Equipment Alone
Reliability	97.36%	98.74%	98.59%
LOLP	2.64%	1.26%	1.41%
LOLF	5792	2763	3085

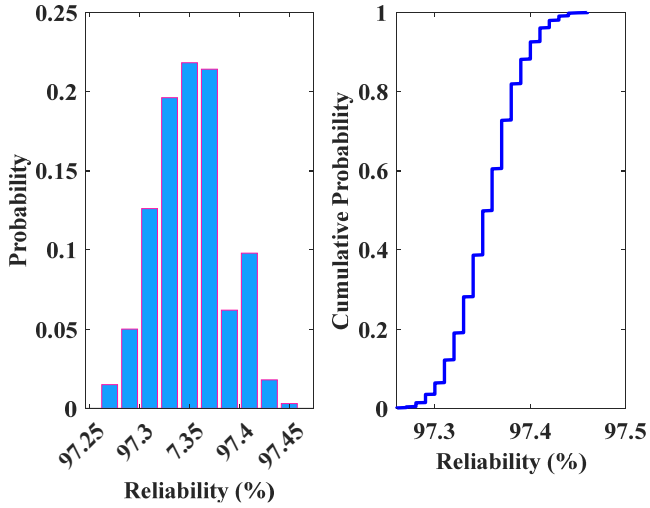

Figure 14. PDF and CDF of SMG system reliability.

4.4. Comparison Between Different Confidence Levels

In summary, the reliability outcomes of this research are as follows: with a 95% confidence interval, the SMG system achieves a reliability of 97.36%; with a 99% confidence interval, reliability decreases to 96.86%; and with a 99.99% confidence interval, reliability further reduces to 95.98%. These results indicate that as the confidence level increases, the reliability of the SMG system decreases. This trend occurs because higher confidence levels encompass a broader range of data and larger confidence intervals, providing a more accurate representation of the true population and capturing greater variability in the data. Consequently, this increased representation of uncertainty leads to a higher likelihood of mismatch between load demand and generation. In other words, the model demonstrates an inverse relationship between resource availability and load demand reliability.

Table 7 presents the reliability values for the SMG system under 99.99%, 99%, and 95% confidence intervals. The system shows a reliability of 97.36% at the 95% confidence interval, which is higher than the values observed at the 99% and 99.99% confidence intervals. This is because increasing the confidence interval widens the range of fluctuations in both energy resources and load demand. As a result, two critical scenarios emerge: high resource availability coupled with low load demand and low resource availability coupled with high load demand. The former positively impacts system reliability, while the latter negatively impacts it. In this simulation, the negative impact dominates, leading to a decrease in reliability. When a higher confidence level (99.99%) is used, more extreme cases are included, further reducing the system's overall reliability. The sensitivity analysis provides additional insights into this behavior.

Table 7. Comparison of SMG system reliability when different confidence intervals are used in the simulation.

	With 99.99% CI	**With 99% CI**	**With 95% CI**
Reliability (mean value)	95.98%	96.86%	97.36%,
Standard deviation	0.0402	0.0345	0.0337
LOLP	4.02%	3.14%	2.64%
LOLF	8814	6886	5792

4.5. Sensitivity Analysis

This section presents several sensitivity studies to examine the impact of uncertainty in both resources and equipment. The confidence interval approach with a 95% confidence level (CI) is employed for the sensitivity analysis in the subsequent subsections.

4.5.1. Load Demand Is Kept Constant

To examine the impact of uncertainty on load demand, the load demand was fixed at both the lower and upper limits throughout the entire 25-year simulation. The results of this analysis are presented in Tables 8 and 9, which show that the uncertainty in load demand led to a 0.24% change in SMG system reliability. This indicates that load demand uncertainty has a relatively minor impact on the system, with only a 0.24% variation in reliability compared to resource uncertainty. The limited impact can be attributed to the use of aggregated load demand data in this study, which results in less fluctuation. Additionally, the load demand data are assumed to be from the previous year (2019), rather than the past 30 years, with 30 random samples generated using a 5% standard deviation. This approach effectively restricts the load fluctuation to a 5% standard deviation, further reducing the variability in the load demand data.

Table 8. Reliability of SMG when load demand is at its minimum.

	SMG System	SMG Resources Alone	SMG Equipment Alone
Reliability	97.43%	98.82%	98.59%
LOLP	2.57%	1.18%	1.41%
LOLF	5624	2584	3083

Table 9. Reliability of SMG when load demand is at its maximum.

	SMG System	SMG Resources Alone	SMG Equipment Alone
Reliability	97.19%	98.57%	98.59%
LOLP	2.81%	1.43%	1.41%
LOLF	6156	3131	3086

4.5.2. Wind Power Generation Is Kept Constant

In this part, wind power generation remains constant over the full 25-year period, both at the upper and lower limits, and the simulation study is repeated in Tables 10 and 11. The goal of this is to study the influence of wind power generating resource uncertainty in the SMG system. These tables indicate that wind resource uncertainty contributes to 22.85% of the changes in reliability. This is understandable, as wind power generation is available around the clock, making it a crucial factor in reducing the loss of load (LOL), especially during night-time when solar power is not available, even in the absence of sufficient battery energy storage.

Table 10. Reliability of SMG when wind power generation is low.

	SMG System	SMG Resources Alone	SMG Equipment Alone
Reliability	75.74%	76.82%	98.59%
LOLP	24.26%	23.18%	1.41%
LOLF	53,126	50,757	3082

Table 11. Reliability of SMG when wind power generation is high.

	SMG System	SMG Resources Alone	SMG Equipment Alone
Reliability	98.59%	100%	98.59%
LOLP	1.41%	0%	1.41%
LOLF	3084	0	3084

4.5.3. Solar Power Generation Is Kept Constant

In this section, the solar power generation is held constant throughout the 25 years, both at the upper and lower limits, and the simulation study is repeated. Tables 12 and 13 present the results of this analysis, revealing that solar power generation uncertainty accounts for only 0.02% of the changes in system reliability. The primary reason for this minimal impact is the insufficient battery energy storage capacity. The subsequent sensitivity analysis further explores this explanation.

Table 12. Reliability of SMG when solar PV is kept at a higher limit.

	SMG System	SMG Resources Alone	SMG Equipment Alone
Reliability	97.40%	98.66%	98.59%
LOLP	2.60%	1.34%	1.41%
LOLF	5688	2937	3083

Table 13. Reliability of SMG when solar PV is kept at a lower limit.

	SMG System	SMG Resources Alone	SMG Equipment Alone
Reliability	97.42%	98.81%	98.59%
LOLP	2.58%	1.19%	1.41%
LOLF	5656	2610	3085

4.5.4. Increment in Battery Capacity by 1 MWh

The previous sensitivity analysis indicated that increasing solar irradiation alone does not significantly improve reliability, suggesting that an abundance of solar energy resources does not necessarily lead to a substantial increase in the SMG system's reliability. To further investigate this, a sensitivity analysis was conducted by adding 1 MWh to the battery energy storage system (BESS) while maintaining the solar PV resources at their maximum capacity. Table 14 demonstrates that adding 1 MWh of BESS, alongside the higher solar irradiation levels, results in a 0.33% increase in reliability. This highlights that the combination of BESS and solar resources can significantly enhance the reliability of the SMG system.

Table 14. Reliability of SMG when the BESS installed capacity is increased.

	SMG System	SMG Resources Alone	SMG Equipment Alone
Reliability	97.69%	99.08%	98.59%
LOLP	2.30%	0.92%	1.41%
LOLF	5046	2011	3082

4.5.5. Consideration of Yearly Load Growth

This section considers a 1% annual increase in load growth for simulation. Table 15 shows that the reliability of the SMG system decreases from 97.36% to 96.19%. Thus, a 1% annual increase in load demand results in a 1.17% reduction in system reliability.

Table 15. Reliability of SMG after 1% increment in annual load demand.

	SMG System	SMG Resources Alone	SMG Equipment Alone
Reliability	96.19%	97.56%	98.59%
LOLP	3.81%	2.44%	1.41%
LOLF	8335	5334	3083

4.5.6. Analyzing the Uncertainty of Equipment Availability

In this study, 1000 Monte Carlo simulation (MCS) runs were conducted for each analysis, with the SMG system reliability varying between 98.51% and 98.66%, resulting in a 0.15% uncertainty due to equipment unavailability. To investigate the effect of increasing the number of simulations, 10,000 MCS runs were performed. As a result, the SMG system reliability now ranges from 98.49% to 98.69%, leading to a 0.20% uncertainty in reliability. The 0.05% difference in reliability between 1000 and 10,000 MCS runs demonstrates that a higher number of simulations more accurately represents the uncertainty associated with equipment availability.

4.6. Comparison Between Confidence Level Approach and CDF Split Method

This study demonstrates that using confidence intervals of 99.99%, 99%, and 95% yields SMG system reliability levels of 95.98%, 96.86%, and 97.36%, respectively. When the CDF split method is applied for reliability evaluation, the system's reliability ranges from a maximum of 98.67% to a minimum of 77.37%. Therefore, when using the confidence interval approach, the SMG system reliability spans from 95.98% to 97.36%, while the CDF split approach results in a broader range, from 77.37% to 98.67%. It can be concluded that the CDF split method has a greater upper limit of SMG system reliability than the confidence interval approach by 1.31%. However, the lowest limit of the confidence interval technique is 18.61% greater than that of the CDF split method.

Table 16 compares the results obtained from the CDF split approach with those from the confidence level approach. It is evident that the confidence level approach offers more intuitive insights through various sensitivity analyses, such as determining the system's reliability under minimal or maximal renewable energy resource availability. In contrast, the CDF split approach provides the reliability values for these 125 scenarios as probabilities, with the 125 datasets being predetermined based on the CDF split concept. This distinction highlights the advantages of the confidence level approach in offering a more flexible and detailed understanding of system performance across different conditions.

Table 16. Comparison of CDF split approach outcome with confidence interval approach outcome.

Reliability of the SMG System	Real-CDF Split Approach	Confidence Interval Approach		
		With Solar Irradiation Uncertainty	With Wind Speed Uncertainty	With Load Demand Uncertainty
Highest possible outcome	98.67%	97.42%	98.59%	97.43%
Lowest possible outcome	77.37%	97.40%	75.74%	97.17%

The CDF split approach offers system reliability as the probability of achieving specific reliability levels, as illustrated in Table 3, a feature that the confidence level approach does not provide. In the design of a 100% renewable energy integrated MG system, a comprehensive analysis of resource availability is crucial. Therefore, it is essential to determine which approach more accurately captures the uncertainty of the variables involved. This ensures that the model used for system reliability assessment appropriately reflects the real-world variability in renewable resource availability, contributing to more robust system design and decision making.

4.7. Selection of Appropriate Approach

If hourly resource availability has remained relatively stable over the last 30 years, the confidence interval approach is appropriate, as it effectively addresses minor fluctuations. However, if there has been significant variation in hourly resource availability during this period, the real-CDF split method is the better option, as the confidence interval approach cannot capture such wide fluctuations. Specifically, the real-CDF split method is suited for

situations where the standard deviation (SD) of hourly climate data over the past 30 years is high, while the confidence interval approach is more appropriate for datasets with lower variability.

In this study, for solar irradiation, the average SD is 0.375%, with a maximum SD of 5.47% and a minimum SD of 0.07%. For wind speed, the average SD is 0.418%, with a maximum SD of 0.77% and a minimum SD of 0.12%. Given these relatively higher standard deviations, the real-CDF split method is recommended for accurately representing resource uncertainty. However, if a dataset from a different SMG system (for instance, from a region with more stable weather conditions) shows a lower SD, such as around 0.05%, the confidence interval approach could be more suitable for that particular system.

5. Conclusions

This research evaluates the reliability of a small-scale microgrid (SMG) over a 25-year operational period, with 2021 serving as the baseline year. It introduces two distinct statistical approaches to incorporate uncertainty in climate data and compares their results. Based on a comprehensive literature review, this study is the first to assess the impact of uncertainty in various simulation approaches on microgrid reliability. It highlights the influence of selecting different confidence levels in reliability evaluation. Additionally, six sensitivity analyses were conducted to support the findings. This study identifies the most suitable statistical approach, alongside the confidence interval method and the cumulative distribution function (CDF) split method, and provides detailed reasoning for its selection. A key conclusion is that the reliability of a microgrid cannot be represented by a single value; instead, it must be expressed as a range, indicating lower and upper bounds. Furthermore, the reliability level should be characterized by the probability of achieving it. While this study conceptualizes the microgrid, practical considerations such as the actual installed capacity of energy resources in an SMG system are not included. The sensitivity analysis reveals that wind power generation has a more significant impact on the SMG's reliability compared to solar PV. To enhance system reliability, the installed capacities of both solar PV and battery energy storage systems need to be increased. Future research will focus on determining optimal ratios between solar PV capacity and battery storage capacity to achieve maximum reliability.

Author Contributions: Conceptualization, S.N.; Methodology, S.N.; Validation, A.A., C.L. and A.M.-S.; Formal analysis, S.N.; Investigation, S.N.; Resources, A.A.; Writing—original draft, S.N. and A.M.-S.; Writing—review & editing, A.A. and C.L.; Supervision, A.A., C.L. and A.M.-S. All authors have read and agreed to the published version of the manuscript.

Funding: This research received no external funding.

Data Availability Statement: The original contributions presented in this study are included in the article. Further inquiries can be directed to the corresponding author(s).

Conflicts of Interest: The authors declare no conflict of interest.

Nomenclature

BESS	Battery Energy Storage System
CDF	Cumulative Distribution Function
CI	Confidence Interval
FTA	Fault Tree Analysis
LOL	Loss of Load
LOLF	Loss of Load Frequency
LOLP	Loss of Load Probability

MCS	Monte Carlo Simulation
MG	Microgrid
MGDN	Microgrid Distribution Network
MRM	Mission Reliability Method
PDF	Probability Distribution Function
PV	Solar Photovoltaic
RBD	Reliability Block Diagram
SD	Standard Deviation
SMG	Standalone Microgrid
TTF	Time to Failure
WT	Wind Turbine

References

1. Faulin, J.; Juan, A.A.; Martorell, S.; Ramírez-Márquez, J.-E. *Simulation Methods for Reliability and Availability of Complex Systems*; Springer: London, UK, 2010.
2. Kennedy, S.; Marden, M.M. Reliability of islanded microgrids with stochastic generation and prioritized load. In Proceedings of the 2009 IEEE Bucharest PowerTech, Bucharest, Romania, 28 June 2009–2 July 2009; IEEE: New York, NY, USA; pp. 1–7.
3. Nallainathan, S.; Arefi, A.; Lund, C.; Mehrizi-Sani, A.; Stephens, D. Reliability Evaluation of Renewable-Rich Microgrids Using Monte Carlo Simulation Considering Resource and Equipment Availability. In Proceedings of the 2020 IEEE International Conference on Power Systems Technology (POWERCON), Bangalore, India, 14–16 September 2020; IEEE: New York, NY, USA; pp. 1–6.
4. Luo, L.; Abdulkareem, S.S.; Rezvani, A.; Miveh, M.R.; Samad, S.; Aljojo, N.; Pazhoohesh, M. Optimal scheduling of a renewable based microgrid considering photovoltaic system and battery energy storage under uncertainty. *J. Energy Storage* **2020**, *28*, 101306. [CrossRef]
5. Shi, X.; Dini, A.; Shao, Z.; Jabarullah, N.H.; Liu, Z. Impacts of photovoltaic/wind turbine/microgrid turbine and energy storage system for bidding model in power system. *J. Clean. Prod.* **2019**, *226*, 845–857. [CrossRef]
6. Qin, Z.; Li, W.; Xiong, X. Incorporating multiple correlations among wind speeds, photovoltaic powers and bus loads in composite system reliability evaluation. *Appl. Energy* **2013**, *110*, 285–294. [CrossRef]
7. Ansari, O.A.; Safari, N.; Chung, C. Reliability assessment of microgrid with renewable generation and prioritized loads. In Proceedings of the 2016 IEEE Green Energy and Systems Conference (IGSEC), Long Beach, CA, USA, 6–7 November 2016; IEEE: New York, NY, USA; pp. 1–6.
8. Karki, R.; Hu, P.; Billinton, R. A simplified wind power generation model for reliability evaluation. *IEEE Trans. Energy Convers.* **2006**, *21*, 533–540. [CrossRef]
9. Sarkar, S.; Ajjarapu, V. MW resource assessment model for a hybrid energy conversion system with wind and solar resources. *IEEE Trans. Sustain. Energy* **2011**, *2*, 383–391. [CrossRef]
10. Karaki, S.; Chedid, R.; Ramadan, R. Probabilistic performance assessment of autonomous solar-wind energy conversion systems. *IEEE Trans. Energy Convers.* **1999**, *14*, 766–772. [CrossRef]
11. Hanna, R.; Disfani, V.R.; Kleissl, J. Reliability evaluation for microgrids using cross-entropy Monte Carlo simulation. In Proceedings of the 2018 IEEE International Conference on Probabilistic Methods Applied to Power Systems (PMAPS), Boise, ID, USA, 24–28 June 2018; IEEE: New York, NY, USA; pp. 1–6.
12. Shi, X.; Bazzi, A.M. Reliability modeling and analysis of a micro-grid with significant clean energy penetration. In Proceedings of the 2015 9th International Conference on Power Electronics and ECCE Asia (ICPE-ECCE Asia), Seoul, Republic of Korea, 1–5 June 2015; IEEE: New York, NY, USA; pp. 202–207.
13. Bie, Z.; Zhang, P.; Li, G.; Hua, B.; Meehan, M.; Wang, X. Reliability evaluation of active distribution systems including microgrids. *IEEE Trans. Power Syst.* **2012**, *27*, 2342–2350. [CrossRef]
14. Yamchi, H.B.; Shahsavari, H.; Kalantari, N.T.; Safari, A.; Farrokhifar, M. A cost-efficient application of different battery energy storage technologies in microgrids considering load uncertainty. *J. Energy Storage* **2019**, *22*, 17–26. [CrossRef]
15. Ghahderijani, M.M.; Barakati, S.M.; Tavakoli, S. Reliability evaluation of stand-alone hybrid microgrid using Sequential Monte Carlo Simulation. In Proceedings of the 2012 Second Iranian Conference on Renewable Energy and Distributed Generation, Tehran, Iran, 6–8 March 2012; IEEE: New York, NY, USA; pp. 33–38.
16. Zhang, H.; Li, Z.; Xue, Y.; Chang, X.; Su, J.; Wang, P.; Guo, Q.; Sun, H. A stochastic bi-level optimal allocation approach of intelligent buildings considering energy storage sharing services. *IEEE Trans. Consum. Electron.* **2024**, *70*, 5142–5153. [CrossRef]

17. Zhai, X.; Li, Z.; Li, Z.; Xue, Y.; Chang, X.; Su, J.; Jin, X.; Wang, P.; Sun, H. Risk-averse energy management for integrated electricity and heat systems considering building heating vertical imbalance: An asynchronous decentralized approach. *Appl. Energy* **2025**, *383*, 125271. [CrossRef]
18. Zhao, J.; Arefi, A.; Borghetti, A.; Ledwich, G. An optimization model for reliability improvement and cost reduction through EV smart charging clean energy. *J. Mod. Power Syst.* **2023**, *12*, 608–620. [CrossRef]
19. Gholami, M.; Arefi, A.; Chowdhury, M.; Ben-Brahim, L.; Muyeen, S. Optimizing transparent photovoltaic integration with battery energy storage systems in greenhouse: A daily light integral-constrained economic analysis considering BESS degradation. *Renew. Energy Focus* **2025**, *53*, 100679. [CrossRef]
20. Hu, H.; Yu, S.S.; Trinh, H. A review of uncertainties in power systems—Modeling, impact, and mitigation. *Designs.* **2024**, *8*, 10. [CrossRef]
21. Polleux, L.; Guerassimoff, G.; Marmorat, J.-P.; Sandoval-Moreno, J.; Schuhler, T. An overview of the challenges of solar power integration in isolated industrial microgrids with reliability constraints. *Renew. Sustain. Energy Rev.* **2022**, *155*, 111955. [CrossRef]
22. Luo, J.; Li, H.; Wang, S. A quantitative reliability assessment and risk quantification method for microgrids considering supply and demand uncertainties. *Appl. Energy* **2022**, *328*, 120130. [CrossRef]
23. Vinothine, S.; Arachchige, L.N.W.; Rajapakse, A.D.; Kaluthanthrige, R. Microgrid energy management and methods for managing forecast uncertainties. *Energies* **2022**, *15*, 8525. [CrossRef]
24. Billinton, R.; Wang, P. Distribution system reliability cost/worth analysis using analytical and sequential simulation techniques. *IEEE Trans. Power Syst.* **1998**, *13*, 1245–1250. [CrossRef]
25. Billinton, R.; Wu, C. Predictive reliability assessment of distribution systems including extreme adverse weather. In Proceedings of the Canadian Conference on Electrical and Computer Engineering 2001. Conference Proceedings (Cat. No. 01TH8555), Toronto, ON, Canada, 13–16 May 2001; IEEE: New York, NY, USA; Volume 2, pp. 719–724.
26. Arefi, A.; Ledwich, G.; Nourbakhsh, G.; Behi, B. A fast adequacy analysis for radial distribution networks considering reconfiguration and DGs. *IEEE Trans. Smart Grid* **2020**, *11*, 3896–3909. [CrossRef]
27. Sakthivelnathan, N.; Arefi, A.; Lund, C.; Mehrizi-Sani, A.; Stephens, D. Marginal Cost of Reliability Improvement for Standalone Microgrids. In Proceedings of the 2021 31st Australasian Universities Power Engineering Conference (AUPEC), Horizon Power, Perth, Australia, 26 September 2021; IEEE: New York, NY, USA; pp. 1–6.
28. Manohar, M.; Koley, E.; Ghosh, S. Microgrid protection under weather uncertainty using joint probabilistic modeling of solar irradiance and wind speed. *Comput. Electr. Eng.* **2020**, *86*, 106684. [CrossRef]
29. Bouchekara, H.R.E.-H.; Javaid, M.S.; Shaaban, Y.A.; Shahriar, M.S.; Ramli, M.A.M.; Latreche, Y. Decomposition based multiobjective evolutionary algorithm for PV/Wind/Diesel Hybrid Microgrid System design considering load uncertainty. *Energy Rep.* **2021**, *7*, 52–69. [CrossRef]
30. Thevenard, D.; Pelland, S. Estimating the uncertainty in long-term photovoltaic yield predictions. *Sol. Energy* **2013**, *91*, 432–445. [CrossRef]
31. Haghifam, S.; Najafi-Ghalelou, A.; Zare, K.; Shafie-khah, M.; Arefi, A. Stochastic bi-level coordination of active distribution network and renewable-based microgrid considering eco-friendly Compressed Air Energy Storage system and Intelligent Parking Lot. *J. Clean. Prod.* **2021**, *278*, 122808. [CrossRef]
32. Nau, R. *Review of Basic Statistics and the Simplest Forecasting Model: The Sample Mean*; Fuqua School of Business, Duke University: Durham, NC, USA, 2014.